Role of PbSe Structural Stabilization in Photovoltaic Cells

*Demet Asil, Brian J. Walker, Bruno Ehrler, Yana Vaynzof, Alessandro Sepe, Sam Bayliss, Aditya Sadhanala, Philip C. Y. Chow, Paul E. Hopkinson, Ullrich Steiner, Neil C. Greenham, and Richard H. Friend**

Semiconductor nanocrystals are promising materials for printed optoelectronic devices, but their high surface areas are susceptible to forming defects that hinder charge carrier transport. Furthermore, correlation of chalcogenide nanocrystal (NC) material properties with solar cell operation is not straightforward due to the disorder often induced into NC films during processing. Here, an improvement in long-range ordering of PbSe NCs symmetry that results from halide surface passivation is described, and the effects on chemical, optical, and photovoltaic device properties are investigated. Notably, this passivation method leads to a nanometer-scale rearrangement of PbSe NCs during ligand exchange, improving the long-range ordering of nanocrystal symmetry entirely with inorganic surface chemistry. Solar cells constructed with a variety of architectures show varying improvement and suggest that triplet formation and ionization, rather than carrier transport, is the limiting factor in singlet fission solar cells. Compared to existing protocols, our synthesis leads to PbSe nanocrystals with surface-bound chloride ions, reduced sub-bandgap absorption and robust materials and devices that retain performance characteristics many hours longer than their unpassivated counterparts.

1. Introduction

Lead chalcogenide nanocrystals (NCs) are important semiconductor materials for visible and infrared photodetectors,[1–5] photovoltaics (PV),[6–11] displays[12,13] and transistors[14,15] but their surfaces are prone to defects that lead to low-energy states in the semiconductor bandgap. In inorganic semiconductors, passivation can reduce defects that are considered to be due to (1) intrinsic NC structure or (2) to opportunistic oxidants. Although evidence suggests that the second of these two defects leads to the greatest loss in performance for semiconductor NCs,[16,17] there is a dearth of techniques for mitigating the defects that arise during ligand substitution and relatively few means to relate NC surface structure with their optoelectronic functionality.[18–21] Recent studies showed that materials that can produce multiple excitons per photon may allow single junction solar cells to exceed the Shockley–Queisser limit.[22–26] In pentacene, for example, singlet exciton fission occurs with high efficiency,[27] creating two triplet excitations on a pair of neighboring molcules that can be ionized with an appropriate acceptor.[23,28,29]

One of the greatest barriers to the use of nanocrystals in photovoltaic devices is their surface chemistry. Through colloidal synthesis, nanocrystal surfaces are terminated with surfactant ligands (e.g., oleic acid) that are insulating,[30] and these ligands can be exchanged after synthesis to improve conductivity.[31,32] One common ligand exchange protocol uses bidentate thiols, such as 1,3-bezenedithiol (BDT), to decrease interparticle spacing, increase conductivity, and increase both short-circuit current and fill factor of films of photovoltaic cells made from PbS and PbSe NCs.[7,15,33,34] However, such ligand exchange techniques generally result in disordered thin films.[35,36] Alternative methods, such as post-synthetic ligand exchange in particle suspensions and colloidal atomic layer deposition have been used with PbSe NCs.[37–40] The first of these is often impractical for devices, and the second results in short-range ordered, fused NCs that have broader size distribution.

Decreasing the intragap state density in semiconductor nanocrystals,[18,41,42] or otherwise improving band alignment,[43–47] has been shown to increase the efficiency of NC solar cells. Halide and metal halide reagents have been used with PbS NCs, resulting in photovoltaic power conversion efficiencies up to 7%.[7,42] However, monovalent halide (Cl^-, Br^-, I^-) exchanged PbS thin films lack order in dot packing, which probably limited the maximum attainable efficiencies.[41] It is known that chloride ions can passivate the surface of CdSe NCs during synthesis,[48,49] and it would be beneficial to adapt this chemistry to materials with higher mobilities[50] and a better ability to harvest the solar spectrum, such as the higher lead chalcogenides.[51] However, these materials are more vulnerable to oxidation due to lower electronegativity of selenium (Se) and tellurium (Te) compared to sulfur (S).[33,52–54] Surprisingly, passivation of PbSe[55–57] and PbTe[58] NCs has attracted less attention than PbS,[59–61] and passivation methods that aim to reduce electronic defects introduced during solid state ligand exchange remain unexplored to date.

D. Asil, Dr. B. J. Walker, Dr. B. Ehrler, Dr. Y. Vaynzof,[+]
Dr. A. Sepe, S. Bayliss, A. Sadhanala, P. C. Y. Chow,
Dr. P. E. Hopkinson,[+] Prof. U. Steiner,
Prof. N. C. Greenham, Prof. R. H. Friend
Cavendish Laboratory
University of Cambridge
J J Thomson Ave, Cambridge CB3 0HE, UK
E-mail: rhf10@cam.ac.uk
[+]Present address: Centre for Advanced Materials, Heidelberg University, Im Neuenheimer Feld 227, Heidelberg 69120, Germany

DOI: 10.1002/adfm.201401816

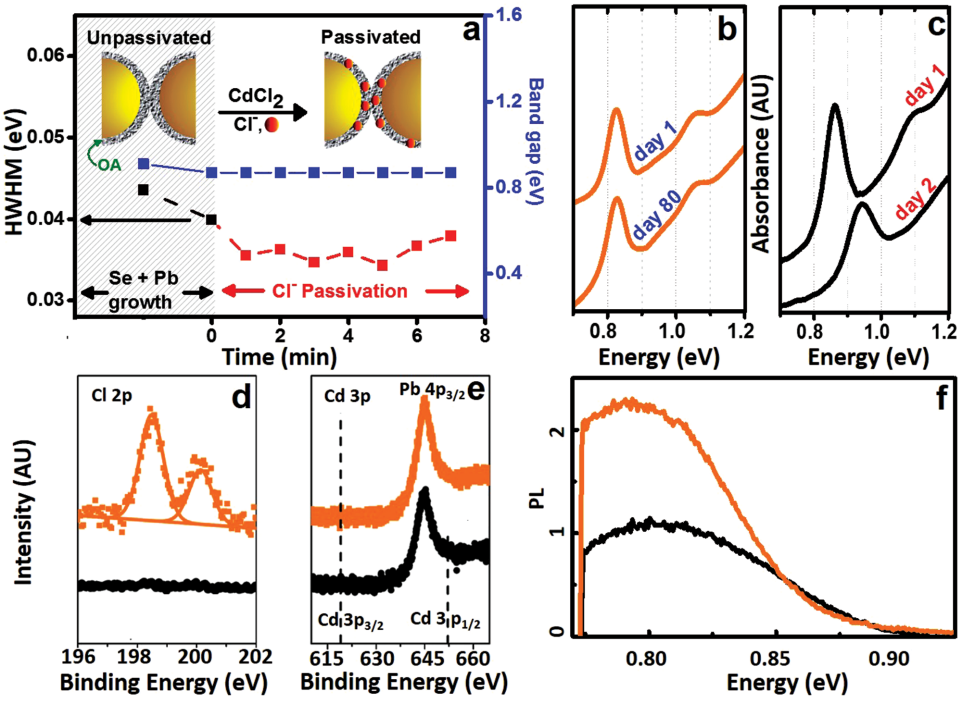

Figure 1. Basic characterization of surface passivation. a) Reaction parameter control during $CdCl_2$ injection. Changes in bandgap (blue) and size distribution (half width at half maximum) (black/red) are shown before and after the $CdCl_2$ injection. Inset: Schematic representation of the NC surface passivation with Cl, which begins after injection of $CdCl_2$ and proceeds for the duration of the reaction (>5 min). b) Absorption spectrum of passivated (orange) PbSe NCs, after 1,3-bezenedithiol (BDT) exchange, shows negligible change after storage in air for 80 days. c) The absorption spectrum of unpassivated (black) PbSe NC film, after BDT exchange, shows significant changes after 2 days in air due to surface oxidation. Spectra offset for clarity. d) Chlorine 2*p* XPS spectrum is pronounced for passivated PbSe NCs (orange) in a BDT-exchanged film. e) Cadmium 3p XPS features are absent for passivated and unpassivated PbSe NCs, indicating that Cd does not participate in surface passivation. f) Photoluminescence of untreated (black) and $CdCl_2$-treated (orange) PbSe films exchanged with BDT. The twofold increase in PL after $CdCl_2$ treatment indicates that nonradiative losses are reduced and that passivation is successful.

Here, we describe a surface passivation method for solvent-dispersed PbSe NCs using cadmium chloride ($CdCl_2$), leading to a well-defined bandgap and enhanced material stability. The conditions are optimized so that passivation occurs through Cl^- ions, and we investigate the properties of NC thin films after ligand exchange in order to assess the effect of the method on solar cells. These PbSe NCs provide a platform to assess the effects on photophysical and material properties, including stability, local and long-range structure, elemental analysis, and performance of interface-sensitive singlet fission sensitized and depleted heterojunction photovoltaic devices. Our passivation treatment leads to better-defined excited state dynamics, structural control, and increased robustness of NCs to atmospheric exposure.

2. Results and Discussion

2.1. Synthesis, Characterization, and Stability of PbSe NCs

We synthesized PbSe NCs using modifications of literature methods. Initial formation of $Pb(oleate)_2$, as well as the reaction with trioctylphosphine selenide to nucleate colloidal PbSe crystallites, were carried out as previously (see Methods Section in Supporting Information for details).[62] To passivate PbSe NCs, we adapted a procedure previously explored for PbS NCs.[41] A solution of $CdCl_2$ in oleylamine and tetradecylphosphonic acid (TDPA) was injected at the conclusion of the growth period. The reaction was incubated at an elevated temperature, and then terminated via rapid dilution with anhydrous hexane. Unpassivated NCs were synthesized and purified through precipitation, but were removed from a cooled reaction vessel after growth (**Figure 1**a).

As shown in Figure 1a, the size distribution of the particles is broad prior to the injection of $CdCl_2$ and quickly narrows to a stable value around a half width at half maximum (HWHM) of 34 meV. For maximum size focusing and minimal Ostwald ripening, the optimum time for terminating the reaction was 5–6 min after $CdCl_2$ injection (Figure 1a). This protocol produced NCs with well-defined 1st, 2nd, and 3rd excitonic transitions[63–65] (Figure S1, Supporting Information). To eliminate the effects of size distribution when comparing passivated and unpassivated samples, we ensured that both NC samples have the same HWHMs (Table S1, Supporting Information).

NCs are generally synthesized with amphiphilic Lewis bases (here oleic acid, OA) that bind to the metal-rich surface and impart colloidal stability.[66–68] A large fraction of the atoms in a NC is at its surface, which is dynamic and crystallographically disordered.[34,69–71] This structural disorder leads to disorder in the electronic structure of NCs immediately after synthesis, and

Adv. Funct. Mater. **2014**,
DOI: 10.1002/adfm.201401816

the low energy states in this distribution can trap charge carriers. In addition to inherent traps that are by-products from synthesis, the reaction of NCs with other Lewis bases introduced during ligand exchange can lead to formation of midgap states. Previous reports showed that BDT ligand exchanged PbSe films are unstable when devices are exposed to ambient conditions.[34,72,73] Hence, the heterogeneity in ligand exchange reactions can lead to a distribution in surface sites, and these can be additional sources of midgap energy states.

We examined the effect of air exposure on BDT-exchanged thin films to test the robustness of our passivation method to opportunistic substitution. Figure 1b,c shows absorption spectra of passivated and unpassivated NC films immediately following ligand exchange with BDT (top), and the same sample measured again after air exposure for a defined interval (bottom). After just two days the absorption spectrum of the unpassivated PbSe thin films blue-shifted (0.1 eV) together with a significant broadening, presumably induced by increased static disorder. This observation is consistent with PbSe surfaces that have lost surface ligands and undergo chemical conversion to higher bandgap species, such as $PbSeO_x$, Pb–O, and/or Pb–OH, resulting in PbSe nanocrystals with a smaller effective size.[74] In contrast, there was no significant shift observed for the passivated PbSe even after 80 days, indicating that the surface passivation technique is an effective means to improve the robustness of PbSe solids.

X-ray photoelectron spectroscopy (XPS) was used to assess the extent of interaction of the surface Pb and Se atoms with the injected $CdCl_2$ solution. As the Pb–Cl bond has a slightly higher binding energy compared to atomically clean Pb, a shift of the Pb 4*f* spectrum to the higher-energy side and development of a new feature between the Pb 4*f* peaks are expected (Figures S2 and S3, Supporting Information).[72,75] The XPS data show 12% Cl composition in passivated PbSe. No change in Se 3*d*, Se 3*p*, and S 2*p* peaks indicates that the described method is not affecting the surface Se and S atoms. Notably, no Cd is detected in either OA or BDT-capped PbSe NCs (Figure S4, Supporting Information). This absence of Cd contrasts with other passivation methods based on $CdCl_2$.[18] However, the result is consistent with previous observations that the main consequence of $CdCl_2$ treatment is the binding of Cl to Pb atoms at the NC surface, and that no Cd is found after NC purification. Here, the lack of Cd incorporation is due to the low temperature injection and the use of a low concentration of Cd, relative to Pb contained in the nanocrystals, during passivation (Cd:Pb; 1/6).[55] At this temperature, Cd is detected only when the passivation reaction contains higher concentrations of $CdCl_2$ (Cd:Pb; 1/4). The change in the final ratio of Pb/Se is and is 2.21 ± 0.03 for both treated and untreated samples, which shows that the surface Se atoms are not etched with the method described here in contrast to the molecular chlorine (Cl_2) treatment described by Bae et al.[72] The absence of Se etching in our method is attributed to the lower oxidative strength of the chloride ions (Cl^-) compared to Cl_2.

FTIR spectra of passivated and unpassivated nanocrystal films are shown in Figure S5, Supporting Information. To assess the surface chemistry, two different film deposition methods were also compared: nanocrystal films that have been drop cast without ligand exchange (i.e., with native oleate ligands, Figure S5a, Supporting Information), and films prepared with a layer-by-layer spin-casting, with alternating ligand exchange with BDT (Figure S5b, Supporting Information). For both a) and b), the pairs of films are prepared with matching film absorption, to ensure that the number of nanocrystals is comparable. Panel (a) shows that passivated nanocrystals, terminated with oleate ligands, have a C–H absorption that is 50% smaller than that of unpassivated nanocrystals with otherwise identical synthesis. Upon treatment and cross-linking with the with the strong Lewis base BDT, both the passivated and unpassivated nanocrystals have similar, low intensity absorptions at the C–H stretch frequency (2900 cm^{-1}). The results suggest that the passivation process acts as a preliminary exchange process at the nanocrystal surface, and this passivation displaces half of the oleate ligands prior to treatment with BDT.[76,77] Hence, we conclude that a large fraction of the native ligands are removed by BDT treatment, likely binding through a thiolate moiety,[66–68,76,77] in agreement with the earlier report on PbS.[7]

In semiconductor NCs, surface defects can lead to nonradiative decay pathways that reduce the quantum efficiency of the band edge PL.[78–80] Although no difference in PL for passivated and unpassivated NCs was seen for dispersed PbSe in octane (see Table S1, Supporting Information, for details), a significant improvement was observed following solid state BDT ligand exchange (Figure 1f). The $CdCl_2$ treatment resulted in a twofold increase in PL intensity. Moreover, the PL linewidth narrows and the PL intensity increases, indicating that passivated nanocrystal films have fewer nonradiative decay channels. Together, our results indicate that passivation reduces the effect of trap states in nanocrystals and plays a significant role during the formation of a well-defined symmetry propagating within the entire nanocrystal film.

2.2. Order and Assembly of PbSe NCs

The extent of superlattice order in nanocrystal films was investigated using grazing incidence small-angle X-ray scattering (GISAXS). These GISAXS data show prominent Bragg reflections at positions that correspond to the *d*-spacing and lattice structure of the film, and by employing a beam cross section footprint on the sample averaging over ≈3 cm length and with an incident angle slightly above the critical angle of the material, the scans sample a large range of q values and are sensitive to structural properties over the entire film volume. In this way, any change in the short- or long-range ordering, occurring in the films' internal structures is probed methodically (**Figure 2**a,b). A comparison between the 2D GISAXS maps of the films before (Figure S6, Supporting Information) and after the ligands exchange reveals that the process induces a change in the morphological structure of the samples, analogous to that observed in refs. [34,81,82]. When compared with the samples after ligand exchange, the 2D GISAXS maps of the as-prepared film have high order Bragg reflections at high q-values. These features indicate that long-range ordering within the nanometer-scale lattice is present. In order to quantify and track any changes occurring within the thin films, intensity profiles were constructed along q_y at the q_z-value where the transmission function of the nanostructured films has a maximum, i.e., at

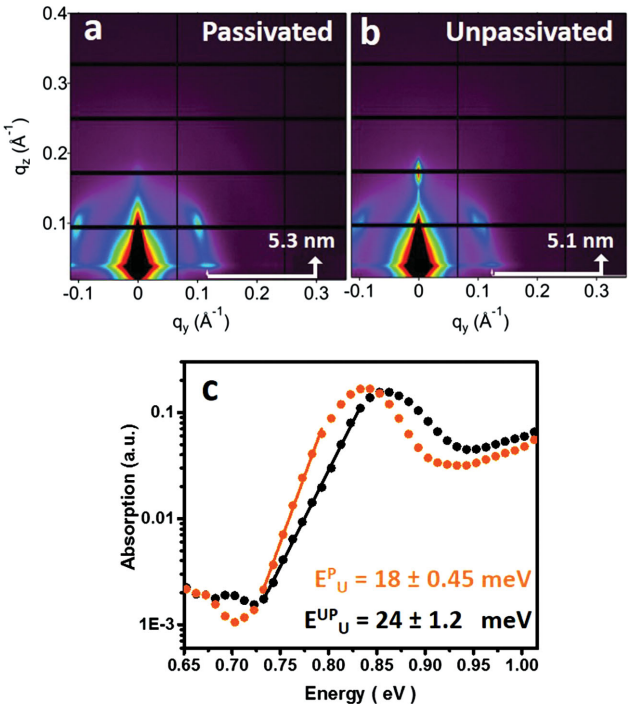

Figure 2. Characterization of the symmetry disorder in PbSe NC films. a) 2D GISAXS map, as a function of the scattering vector q, of a) passivated b) unpassivated BDT exchanged thin films, taken at an incident angle $\alpha_i = 0.15°$. GISAXS map demonstrates the propagation of a defect free structure with a well-defined symmetry in passivated films. The sizes of the passivated and unpassivated NCs are 4.5 and 4.3 nm, respectively. c) Photothermal deflection spectrum of passivated (orange) and unpassivated (black), BDT exchanged thin films. Solid lines represent the linear fit of the slope. The Urbach energy (E_U) is measured for the passivated and unpassivated, BDT-exchanged NC films as shown (including the fitting error of ±5%). The passivated PbSe films shows somewhat less disorder compared to unpassivated PbSe.

0.027 Å^{-1} for the as-prepared and 0.038 Å^{-1} for the passivated and unpassivated ligand exchanged films.

In Figure 2a,b, the main differences between the structures of films composed of unpassivated versus passivated nanocrystal thin films are the loss of intensity in vertical scattering features (≈0.17 Å^{-1}) and gain in lateral features (≈0.12 Å^{-1}). These changes imply that surface passivation causes changes in the geometrical lattice arrangement of the particles in thin films. Two peaks are present at $q_z \approx 0.095$ A^{-1} in the case of the unpassivated film, meanwhile after passivation only a single peak is present, thus the passivated thin film presents a very well defined suprasymmetry in contrast with the unpassivated crystals, where a mixed suprasymmetry is instead present. Therefore, we conclude that the passivation affects the symmetry and changes the packing of the NCs in coupled films. The center-to-center distance is measured as 6 nm for OA-capped PbSe which results in 1.7 nm spacing between particles. A significant decrease is indicated following the ligand exchange with BDT. However, the interparticle spacing is not affected by the $CdCl_2$ passivation. Excluding the size of the particles, the interparticle spacing is 0.8 nm for the BDT ligand-exchanged passivated and unpassivated PbSe NCs. This decreased spacing indicates that the inorganic surface composition is driving the ordered self-assembly of particles, and extends the self-assembly observed for sparse nanostructures in other contexts[83–85] to a close-packed nanocrystal lattice.

Photothermal deflection spectra (PDS) for passivated and unpassivated NC films are shown in Figure 2c. PDS is a powerful technique to determine transitions well below the optical bandgap. A detailed description of the PDS setup can be found in Kronemeijer et al.[86] In inorganic semiconductors, disorder is known to result in the formation of states in the bandgap, broadening of the absorption onset and creating an exponential sub-bandgap absorption tail called the Urbach tail.[87] The characteristic width of the exponential absorption tail, the Urbach energy (E_U), correlates with the amount of energetic disorder in the material.[88,89] As the effect due to the dissimilar polydispersity values has been eliminated (see Table S1, Supporting Information), the difference in E_U is directly attributed to differences in the amount of disorder in the material. Here, E_U is calculated to be 18 ± 0.45 meV and 24 ± 1.2 meV for the passivated and unpassivated PbSe NCs, respectively, indicating that the passivation process reduces the energetic disorder in ligand-exchanged PbSe films. Additional measurements on smaller PbSe NCs with a 1.35 eV bandgap show that the effect of passivation is more significant for smaller NCs. PDS spectra for passivated and unpassivated PbSe NCs having 28 and 29 meV HWHM values and 1.35 eV bandgap are shown in Figure S7, Supporting Information. The Urbach energy decreases from 38.7 ± 1.9 to 25 ± 1.3 meV with the passivation method described in the study.

2.3. Excited State Dynamics

The excited state dynamics of NCs were assessed by transient absorption (TA) spectroscopy.[90–92] **Figure 3** shows the time progression of the TA spectra. The most evident signal is the ground state bleach (GSB) at around 0.85 eV. As in the ground state absorption spectrum, the narrow size distribution of NCs leads to a narrow ground state bleach in TA. There is a 50 nm shift in the GSB position in accordance with the 0.03 eV shift in their absorption maxima. It is also apparent that the GSB of the passivated NCs decays with a well-defined lifetime, which agrees well with the luminescence lifetime observed in other spectroscopic experiments on PbSe NCs.[93–97] In Figure 3b, however, the corresponding GSB of the unpassivated NCs has a component that persists for longer than 10 µs. We summarize the kinetics for these bleach signatures in Figure 3c. To interpret the differences in the TA signals, we consider the origin of the ground state bleach in this sample. Because all PbSe NCs have a common ground state, the ground state bleach is a signature of all of the excited PbSe species regardless of the specific identity of these excited states. There is no barrier to exciton dissociation in these films, but due to the lack of a heterojunction there is also no impetus for long-range charge separation. It is also evident that the long-lived species does not form in PbSe NCs that have been treated with $CdCl_2$; in these samples, the lifetime is consistent with band-to-band recombination.[98] Hence, we attribute the long-lived excited state species to carriers that have been trapped through defect-related states near the NC surface.

Adv. Funct. Mater. **2014**,
DOI: 10.1002/adfm.201401816

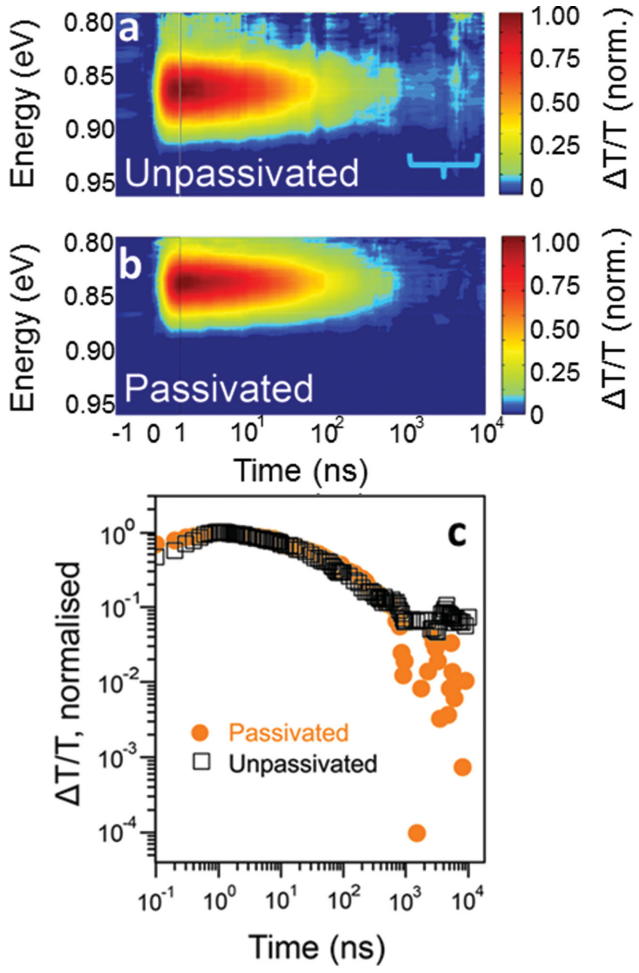

Figure 3. Transient absorption spectra, normalized, -of thin films of a) unpassivated and b) passivated PbSe NCs, treated with BDT. The effect of trapping is observed as a persistent excited state population that bleaches the $1S_e$–$1S_h$ transition, which is not present in NCs that have been passivated with $CdCl_2$. c) Transient absorption kinetics of the $1S_e$–$1S_h$ ground state bleach for thin films of unpassivated (black squares) and passivated (orange dots) PbSe NCs, treated with BDT. The passivated NCs decay with a lifetime of 300 ns. The unpassivated NCs have a persistent slow component attributed to trapped species.

2.4. Effect of Structural Stabilization on Photovoltaic Cells

Among the most efficient PbSe solar cells reported to date are hybrid bilayer solar cells made from PbSe NCs and the organic singlet fission sensitizer pentacene.[29] We therefore fabricated PbSe/pentacene bilayer solar cells to investigate the effect of surface passivation on the long-term stability of these devices. In singlet fission, a spin-singlet exciton on an organic chromophore relaxes to a pair of lower-energy triplet excitons.[99] As represented in Figure S8, Supporting Information, pentacene absorbs high energy photons, then undergoes singlet fission within 80 fs.[100] PbSe, on the other hand, absorbs infrared (IR) photons and acts as an electron acceptor.[23,28] Compared to previous PbSe devices,[29] the open-circuit voltage (V_{OC}) of our photovoltaic cells with unpassivated PbSe is 25% higher (see Table S2, Supporting Information, for details). This increase in V_{OC} is significant, and we attribute it to the narrower size distribution of NCs in this work compared to those reported previously.[29] In order to discriminate the effect of passivation, we fabricated independent devices, each using passivated or unpassivated NCs with identical size distributions. The V_{OC} of the passivated and unpassivated samples are comparable within experimental error; hence the passivation method described here has little direct effect on *V*oc (see Figure S9, Supporting Information). In devices with passivated NCs we observe a significant enhancement in FF, consistent with more homogeneous percolation networks for charge carrier transport and with higher order and symmetry[101] as characterized by our PDS and GISAXS measurements. The main contribution to the difference in FF was 50% decrease in the device series when passivated nanocrystals were used instead of unpassivated nanocrystals (Table S2, Supporting Information).

To assess device stability, we conducted longitudinal studies of devices under continuous solar exposure in air. The change in device parameters is shown in **Figure 4**a,b; for unpassivated samples, there is a rapid initial drop in FF and hence power conversion efficiency (PCE). In contrast, solar cells prepared with passivated NCs retained over 95% of the FF after 2 h, and 90% after 10 h. This device stability is analogous to that observed for the optical characterization above (Figure 1) and is related to the decreased vulnerability of the passivated PbSe thin films to oxidation.

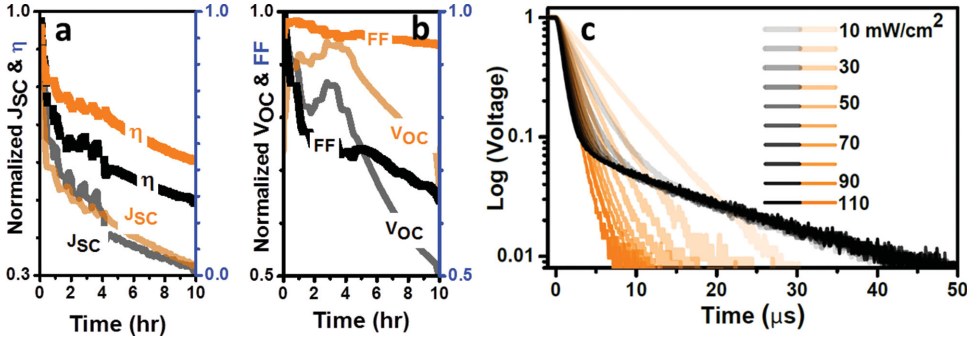

Figure 4. Device stability and transient photovoltage characteristics. a) Change in η and J_{SC} and b) change in V_{OC} and FF under continuous solar irradiation for 10 h (see Figure S11, Supporting Information, for separate plots). c) Transient photovoltage measurements of unpassivated (black) and passivated (orange) PbSe NCs under white light bias (data are normalized). Unpassivated NCs decay independently of light power with a bi-exponential kinetic attributed to trap assisted recombination. Passivated NCs show mono-exponential decay.

The surface treatment and stabilization of PbSe NCs modestly improves the PCE of singlet fission-sensitised solar cells (Table S2, Supporting Information). To explore the origin of this increase, we conducted transient photovoltage measurements, which measure the decay of photogenerated voltage after the absorption of an excitation pulse.[102] Hence, this technique is an efficient probe of recombination channels in phototvoltaic devices. The singlet fission-sensitised devices with passivated PbSe NCs showed mono-exponential decays (Figure 4c), indicating that all carriers decay via a single channel. In contrast, the unpassivated NC devices showed a bi-exponential behavior with a longer decay timescale independent of white-light bias for about 10% of the population. We emphasize that the persistent, long-lived photovoltage for unpassivated NC solar cells agrees exactly with the long-lived excited state population observed in transient absorption of unpassivated PbSe films (Figure 3c).

To explore the chief limiting factors of these singlet fission solar cells, we repeated these experiments with all-inorganic photovoltaic devices in a depleted heterojunction architecture, containing NCs with different bandgaps. The results are represented in Figure S10 and Table S3, Supporting Information. Devices that contained passivated nanocrystals with a bandgap of 1.35 eV showed a 23% higher J_{SC}, and 34% higher power conversion efficiency, than devices with unpassivated nanocrsytals of the same size. The effect of passivation is far larger for smaller NCs (E_g = 1.35 eV) than those with larger nanocrystals (E_g = 0.85 eV), and suggests that the number of traps that can be passivated increases with the relative surface area, and presumably with the trap state density, of the particles.[103]

A comparison of these two devices also shows the limitations on device operation. Despite the success of the surface passivation in eliminating long-lived species in TA and transient photovoltage, the performance of the devices does not improve significantly. Instead, the dominant effect of passivation on device performance is to preserve their relatively favourable transport properties. This analysis suggests that the chief limitation in singlet fission devices is the yield of triplet formation, transfer and ionisation, and subsequent carrier transport, near the NC interface.

3. Conclusions

The controlled passivation method described here allowed us to synthesize trap-free and air-stable PbSe NCs. Injection of $CdCl_2$ immediately after the NC growth period leads to passivation by Cl^- and reduction in NC size distribution. We found that passivated PbSe thin films exhibit lower trap density, leading to higher PL intensity and a shorter excited state lifetime. The change in inter-NC interaction induced a well-defined symmetry within the film, as the supracrystallinity of NCs reorients the symmetry of close-packed particles. Passivated PbSe surfaces gave rise to reduced energetic disorder versus their unpassivated counterparts, as reflected by the decrease in the Urbach energy. Transient absorption and bi-exponential decay kinetics in transient photovoltage measurements identified the presence of a slow, trapped-carrier recombination channel in unpassivated devices which are persistent for longer than 10^{-5} s and are responsible for 10% of the decay of charges. Passivation of PbSe eliminated this slow recombination channel.

Finally, we fabricated multiple photovoltaic architectures to identify the chief limitations to NC device design. Further studies to improve singlet fission-sensitised solar cells will focus on increasing the singlet fission yield, tuning the interface between organic and inorganic seminconductors, and uncovering the surface chemical basis for the structural reorientation. Most promising of all, these surface passivation methods enhance the long-term material and device stability of PbSe, while also inducing significant long-range structural stabilization. This surface passivation method and its variations are thus expected to be broadly significant for the chemical and material robustness of low-dimensional semiconductors.

4. Experimental Section

Methods: A Perkin-Elmer Lambda 9 UV–vis-NIR spectrometer was used to monitor the reaction and first excitonic peaks by taking small aliquots while the reaction proceeds. The solution measurements were done in tetrachloroethyelene and thin film measurements were done by spin coating several layers of PbSe with or without BDT ligand exchange onto Spectrosil discs. The thin films on Spectrosil were used for photothermal deflection spectroscopy (PDS), transient absorption spectroscopy (TAS), and photoluminesence (PL) measurements. Thin-film samples were prepared on 10 nm gold-coated silicon for XPS and on bare silicon for GISAXS in the same way as described above. The photoluminescence spectra were measured using a thermoelectrically cooled InGaAs array CCD camera (iDus, Andor) coupled with an imaging spectrograph (Shamrock 303i, Andor), and were corrected for detector response. The samples were photoexcited with the 808 nm output of a diode laser (IQu1C, Laser 2000 Ltd.).

Device Fabrication and Characterization: ITO (Psiotec) was cleaned in acetone and isopropyl alcohol for 15 min and dried under a nitrogen stream. After plasma etching of the cleaned ITO substrates, 50 nm pentacene was evaporated at pressures as low as 10–7 mbar. PbSe was spin coated on top of fresh pentacene films by the layer-by-layer (L-B-L) procedure. Briefly, PbSe (30 mg mL^{-1} in octane), 1,3 benzene-1,3-dithiol (3 vol% in acetonitrile), acetonitrile, and octane were subsequently spin coated at 1500 rpm for 7 s after 3 s soaking time. The devices were loaded into a thermal evaporator in order to evaporate LiF (1 nm) and Al (100 nm) as cathode. Finally, the devices were completed by encapsulation. Devices were characterized under an Oriel 92250A solar simulator after correcting the incident power for spectral mismatch. Current–voltage measurements were performed by a Keithley 2636A sourcemeter unit and external quantum efficiency spectra were recorded under monochromatic light from an Oriel Cornerstone 260 monochromator.

Supporting Information

Supporting Information is available from the Wiley Online Library or from the author.

Acknowledgements

D.A. and B.J.W. contributed equally to this work. The authors acknowledge support from the Engineering and Physical Sciences Resources Council and a Pump-Prime Grant from the Winton Programme for the Physics of Sustainability. Middle East Technical University, Turkish Council of Higher Education, and Schlumberger-Faculty for the Future Fellowship program supported D. Asil. B.J.W. was

DOI: 10.1002/adfm.201401816

supported by a Herchel Smith Research Fellowship. B.E. acknowledges KACST and Selwyn College Cambridge for funding. A.S. and U.S. acknowledge the European Commission (NMP4-SL20010–246123) for funding. GISAXS measurements are based upon research conducted at beamline I07 at the Diamond Light Source, Didcot, UK. The authors thank S.-H. Liu, K. Sarkar, E. Braden, C. Nicklin, and J. Rawle for their help during the I07 experiment at Diamond Light Source.

Received: June 4, 2014
Revised: November 26, 2014
Published online:

[1] V. Sukhovatkin, S. Hinds, L. Brzozowski, E. H. Sargent, *Science* **2009**, *324*, 1542.
[2] G. Konstantatos, J. Clifford, L. Levina, E. H. Sargent, *Nat. Photonics* **2007**, *1*, 531.
[3] G. Konstantatos, I. Howard, A. Fischer, S. Hoogland, J. Clifford, E. Klem, L. Levina, E. H. Sargent, *Nature* **2006**, *442*, 180.
[4] J. P. Clifford, G. Konstantatos, K. W. Johnston, S. Hoogland, L. Levina, E. H. Sargent, *Nat. Nanotechnol.* **2009**, *4*, 40.
[5] T. P. Osedach, N. Zhao, S. M. Geyer, L.-Y. Chang, D. D. Wanger, A. C. Arango, M. C. Bawendi, V. Bulovi , *Adv. Mater.* **2010**, *22*, 5250.
[6] I. Gur, N. A. Fromer, M. L. Geier, A. P. Alivisatos, *Science* **2005**, *310*, 462.
[7] A. H. Ip, S. M. Thon, S. Hoogland, O. Voznyy, D. Zhitomirsky, R. Debnath, L. Levina, L. R. Rollny, G. H. Carey, A. Fischer, K. W. Kemp, I. J. Kramer, Z. Ning, A. J. Labelle, K. W. Chou, A. Amassian, E. H. Sargent, *Nat. Nanotechnol.* **2012**, *7*, 577.
[8] D. D. Wanger, R. E. Correa, E. a. Dauler, M. G. Bawendi, *Nano Lett.* **2013**, *13*, 5907.
[9] K. S. Leschkies, T. J. Beatty, M. S. Kang, D. J. Norris, E. S. Aydil, *ACS Nano* **2009**, *3*, 3638.
[10] J. Jean, S. Chang, P. R. Brown, J. J. Cheng, P. H. Rekemeyer, M. G. Bawendi, S. Gradečak, V. Bulović, *Adv. Mater.* **2013**, *25*, 2790.
[11] L.-Y. Chang, R. R. Lunt, P. R. Brown, V. Bulović, M. G. Bawendi, *Nano Lett.* **2013**, *13*, 994.
[12] B. S. Mashford, M. Stevenson, Z. Popovic, C. Hamilton, Z. Q. Zhou, C. Breen, J. Steckel, V. Bulovic, M. Bawendi, S. Coe-Sullivan, P. T. Kazlas, *Nat. Photonics* **2013**, *7*, 407.
[13] M. J. Panzer, V. Wood, S. M. Geyer, M. G. Bawendi, V. Bulovic, *J. Disp. Technol.* **2010**, *6*, 90.
[14] J.-H. Choi, A. T. Fafarman, S. J. Oh, D.-K. Ko, D. K. Kim, B. T. Diroll, S. Muramoto, J. G. Gillen, C. B. Murray, C. R. Kagan, *Nano Lett.* **2012**, *12*, 2631.
[15] Y. Liu, M. Gibbs, J. Puthussery, S. Gaik, R. Ihly, H. W. Hillhouse, M. Law, *Nano Lett.* **2010**, *10*, 1960.
[16] J. I. Saari, E. A. Dias, D. Reifsnyder, M. M. Krause, B. R. Walsh, C. B. Murray, P. Kambhampati, *J. Phys. Chem. B* **2013**, *117*, 4412.
[17] A. Hassinen, I. Moreels, K. De Nolf, P. F. Smet, J. C. Martins, Z. Hens, *J. Am. Chem. Soc.* **2012**, *134*, 20705.
[18] K. Katsiev, A. H. Ip, A. Fischer, I. Tanabe, X. Zhang, A. R. Kirmani, O. Voznyy, L. R. Rollny, K. W. Chou, S. M. Thon, G. H. Carey, X. Cui, A. Amassian, P. Dowben, E. H. Sargent, O. M. Bakr, *Adv. Mater.* **2014**, *26*, 937.
[19] D. Bozyigit, V. Wood, *J. Mater. Chem. C* **2014**.
[20] J. Mooney, M. Krause, J. Saari, P. Kambhampati, *Phys. Rev. B* **2013**, *87*, 081201.
[21] M. I. Bodnarchuk, E. V Shevchenko, D. V Talapin, *J. Am. Chem. Soc.* **2011**, *133*, 20837.
[22] O. E. Semonin, J. M. Luther, S. Choi, H.-Y. Chen, J. Gao, A. J. Nozik, M. C. Beard, *Science* **2011**, *334*, 1530.
[23] B. Ehrler, M. W. B. Wilson, A. Rao, R. H. Friend, N. C. Greenham, *Nano Lett.* **2012**, *12*, 1053.
[24] M. C. Beard, J. M. Luther, O. E. Semonin, A. J. Nozik, *Acc. Chem. Res.* **2013**, *46*, 1252.
[25] A. G. Midgett, J. M. Luther, J. T. Stewart, D. K. Smith, L. A. Padilha, V. I. Klimov, A. J. Nozik, M. C. Beard, *Nano Lett.* **2013**, *13*, 3078.
[26] D. N. Congreve, J. Lee, N. J. Thompson, E. Hontz, S. R. Yost, P. D. Reusswig, M. E. Bahlke, S. Reineke, T. Van Voorhis, M. a. Baldo, *Science* **2013**, *340*, 334.
[27] A. Rao, M. W. B. Wilson, J. M. Hodgkiss, S. Albert-Seifried, H. Bässler, R. H. Friend, *J. Am. Chem. Soc.* **2010**, *132*, 12698.
[28] P. J. Jadhav, P. R. Brown, N. Thompson, B. Wunsch, A. Mohanty, S. R. Yost, E. Hontz, T. Van Voorhis, M. G. Bawendi, V. Bulović, M. A. Baldo, *Adv. Mater.* **2012**, *24*, 6169.
[29] B. Ehrler, B. J. Walker, M. L. Böhm, M. W. B. Wilson, Y. Vaynzof, R. H. Friend, N. C. Greenham, *Nat. Commun.* **2012**, *3*, 1019.
[30] D. Yu, C. Wang, P. Guyot-Sionnest, *Science* **2003**, *300*, 1277.
[31] M. Jarosz, V. Porter, B. Fisher, M. Kastner, M. Bawendi, *Phys. Rev. B* **2004**, *70*, 195327.
[32] V. J. Porter, S. Geyer, J. E. Halpert, M. A. Kastner, M. G. Bawendi, *J. Phys. Chem. C* **2008**, *112*, 2308.
[33] I. J. Kramer, E. H. Sargent, *Chem. Rev.* **2014**, *114*, 863.
[34] J. M. Luther, M. Law, Q. Song, C. L. Perkins, M. C. Beard, A. J. Nozik, *ACS Nano* **2008**, *2*, 271.
[35] T. Hanrath, J. J. Choi, D.-M. Smilgies, *ACS Nano* **2009**, *3*, 2975.
[36] T. S. Mentzel, D. D. Wanger, N. Ray, B. J. Walker, D. Strasfeld, M. G. Bawendi, M. A. Kastner, *Nano Lett.* **2012**, *12*, 4404.
[37] W. J. Baumgardner, K. Whitham, T. Hanrath, *Nano Lett.* **2013**, *13*, 3225.
[38] S. J. Oh, N. E. Berry, J.-H. Choi, E. A. Gaulding, H. Lin, T. Paik, B. T. Diroll, S. Muramoto, C. B. Murray, C. R. Kagan, *Nano Lett.* **2014**, *14*, 1559.
[39] A. Dong, X. Ye, J. Chen, Y. Kang, T. Gordon, J. M. Kikkawa, C. B. Murray, *J. Am. Chem. Soc.* **2011**, *133*, 998.
[40] A. R. Clapp, I. L. Medintz, H. T. Uyeda, B. R. Fisher, E. R. Goldman, M. G. Bawendi, H. Mattoussi, *J. Am. Chem. Soc.* **2005**, *127*, 18212.
[41] J. Tang, K. W. Kemp, S. Hoogland, K. S. Jeong, H. Liu, L. Levina, M. Furukawa, X. Wang, R. Debnath, D. Cha, K. W. Chou, A. Fischer, A. Amassian, J. B. Asbury, E. H. Sargent, *Nat. Mater.* **2011**, *10*, 765.
[42] S. M. Thon, A. H. Ip, O. Voznyy, L. Levina, K. W. Kemp, G. H. Carey, S. Masala, E. H. Sargent, *ACS Nano* **2013**, *7*, 7680.
[43] P. R. Brown, R. R. Lunt, N. Zhao, T. P. Osedach, D. D. Wanger, L.-Y. Chang, M. G. Bawendi, V. Bulovi , *Nano Lett.* **2011**, *11*, 2955.
[44] P. R. Brown, D. Kim, R. R. Lunt, N. Zhao, M. G. Bawendi, J. C. Grossman, V. Bulovic, *ACS Nano*, **2014**, *8*, 5863.
[45] R. L. Z. Hoye, B. Ehrler, M. L. Böhm, D. Muñoz-Rojas, R. M. Altamimi, A. Y. Alyamani, Y. Vaynzof, A. Sadhanala, G. Ercolano, N. C. Greenham, R. H. Friend, J. L. MacManus-Driscoll, K. P. Musselman, *Adv. Energy Mater.* **2014**.
[46] B. Ehrler, K. P. Musselman, M. L. Böhm, F. S. F. Morgenstern, Y. Vaynzof, B. J. Walker, J. L. Macmanus-Driscoll, N. C. Greenham, *ACS Nano* **2013**, *7*, 4210.
[47] C.-H. M. Chuang, P. R. Brown, V. Bulovi , M. G. Bawendi, *Nat. Mater.* **2014**, *13*, 796.
[48] J. S. Owen, J. Park, P. Trudeau, A. P. Alivisatos, *J. Am. Chem. Soc.* **2008**, *130*, 12279.
[49] N. C. Anderson, J. S. Owen, *Chem. Mater.* **2013**, *25*, 69.
[50] G. M. Akselrod, F. Prins, L. V Poulikakos, E. M. Y. Lee, M. C. Weidman, A. J. Mork, A. P. Willard, V. Bulovi , W. A. Tisdale, *Nano Lett.* **2014**.
[51] Y. Liu, J. Tolentino, M. Gibbs, R. Ihly, C. L. Perkins, Y. Liu, N. Crawford, J. C. Hemminger, M. Law, *Nano Lett.* **2013**, *13*, 1578.
[52] J. Zhang, J. Gao, E. M. Miller, J. M. Luther, M. C. Beard, *ACS Nano* **2013**, *8*, 614.

[53] M. H. Zarghami, Y. Liu, M. Gibbs, E. Gebremichael, C. Webster, M. Law, *ACS Nano* **2010**, *4*, 2475.
[54] B. K. Hughes, D. A. Ruddy, J. L. Blackburn, D. K. Smith, M. R. Bergren, A. J. Nozik, J. C. Johnson, M. C. Beard, *ACS Nano* **2012**, *6*, 5498.
[55] J. M. Pietryga, D. J. Werder, D. J. Williams, J. L. Casson, R. D. Schaller, V. I. Klimov, J. A. Hollingsworth, *J. Am. Chem. Soc.* **2008**, *130*, 4879.
[56] P. K. Jain, L. Amirav, S. Aloni, A. P. Alivisatos, *J. Am. Chem. Soc.* **2010**, *132*, 9997.
[57] M. Casavola, M. A. van Huis, S. Bals, K. Lambert, Z. Hens, D. Vanmaekelbergh, *Chem. Mater.* **2012**, *24*, 294.
[58] K. Lambert, B. De Geyter, I. Moreels, Z. Hens, *Chem. Mater.* **2009**, *21*, 778.
[59] J. M. Luther, H. Zheng, B. Sadtler, A. P. Alivisatos, *J. Am. Chem. Soc.* **2009**, *131*, 16851.
[60] Y. Justo, B. Goris, J. S. Kamal, P. Geiregat, S. Bals, Z. Hens, *J. Am. Chem. Soc.* **2012**, *134*, 5484.
[61] B. J. Beberwyck, Y. Surendranath, A. P. Alivisatos, *J. Phys. Chem. C* **2013**, *117*, 19759.
[62] J. S. Steckel, B. K. H. Yen, D. C. Oertel, M. G. Bawendi, *J. Am. Chem. Soc.* **2006**, *128*, 13032.
[63] M. T. Trinh, A. J. Houtepen, J. M. Schins, J. Piris, L. D. A. Siebbeles, *Nano Lett.* **2008**, *8*, 2112.
[64] P. Liljeroth, P. van Emmichoven, S. Hickey, H. Weller, B. Grandidier, G. Allan, D. Vanmaekelbergh, *Phys. Rev. Lett.* **2005**, *95*, 086801.
[65] J. J. Peterson, L. Huang, C. Delerue, G. Allan, T. D. Krauss, *Nano Lett.* **2007**, *7*, 3827.
[66] L. C. Cass, M. Malicki, E. A. Weiss, *Anal. Chem.* **2013**, *85*, 6974.
[67] N. C. Anderson, M. P. Hendricks, J. J. Choi, J. S. Owen, *J. Am. Chem. Soc.* **2013**, *135*, 18536.
[68] L. M. Wheeler, N. R. Neale, T. Chen, U. R. Kortshagen, *Nat. Commun.* **2013**, *4*, 2197.
[69] P. T. Erslev, H.-Y. Chen, J. Gao, M. C. Beard, A. J. Frank, J. van de Lagemaat, J. C. Johnson, J. M. Luther, *Phys. Rev. B* **2012**, *86*, 155313.
[70] M. T. Frederick, J. L. Achtyl, K. E. Knowles, E. A. Weiss, F. M. Geiger, *J. Am. Chem. Soc.* **2011**, *133*, 7476.
[71] V. Petkov, I. Moreels, Z. Hens, Y. Ren, *Phys. Rev. B* **2010**, *81*, 241304.
[72] W. K. Bae, J. Joo, L. A. Padilha, J. Won, D. C. Lee, Q. Lin, W. Koh, H. Luo, V. I. Klimov, J. M. Pietryga, *J. Am. Chem. Soc.* **2012**, *134*, 20160.
[73] K. S. Leschkies, M. S. Kang, E. S. Aydil, D. J. Norris, *J. Phys. Chem. C* **2010**, *114*, 9988.
[74] I. Moreels, B. Fritzinger, J. C. Martins, Z. Hens, *J. Am. Chem. Soc.* **2008**, *130*, 15081.
[75] P. G. Blake, A. F. Carley, V. Di Castro, M. W. Roberts, *J. Chem. Soc. Faraday Trans. 1 Phys. Chem. Condens. Phases* **1986**, *82*, 723.
[76] J. C. Love, L. A. Estroff, J. K. Kriebel, R. G. Nuzzo, G. M. Whitesides, *Chem. Rev.* **2005**, *105*, 1103.
[77] H. Häkkinen, *Nat. Chem.* **2012**, *4*, 443.
[78] R. Bose, J. F. Mcmillan, J. Gao, K. M. Rickey, C. J. Chen, D. V Talapin, C. B. Murray, C. W. Wong, **2008**.
[79] C. R. Kagan, C. B. Murray, M. Nirmal, M. G. Bawendi, *Phys. Rev. Lett.* **1996**, *76*, 1517.
[80] C. R. Kagan, C. B. Murray, M. G. Bawendi, *Phys. Rev. B* **1996**, *54*, 8633.
[81] M. Law, J. M. Luther, Q. Song, B. K. Hughes, C. L. Perkins, A. J. Nozik, *J. Am. Chem. Soc.* **2008**, *130*, 5974.
[82] T. Hanrath, J. J. Choi, D.-M. Smilgies, *ACS Nano* **2009**, *3*, 2975.
[83] R. D. Robinson, B. Sadtler, D. O. Demchenko, C. K. Erdonmez, L.-W. Wang, A. P. Alivisatos, *Science* **2007**, *317*, 355.
[84] C. Schliehe, B. H. Juarez, M. Pelletier, S. Jander, D. Greshnykh, M. Nagel, A. Meyer, S. Foerster, A. Kornowski, C. Klinke, H. Weller, *Science* **2010**, *329*, 550.
[85] M. Fayette, R. D. Robinson, *J. Mater. Chem. A* **2014**, *2*, 5965.
[86] A. J. Kronemeijer, V. Pecunia, D. Venkateshvaran, M. Nikolka, A. Sadhanala, J. Moriarty, M. Szumilo, H. Sirringhaus, *Adv. Mater.* **2013**, *26*, 728.
[87] F. Urbach, *Phys. Rev.* **1953**, *92*, 1324.
[88] R. A. Street, *Hydrogenated Amorphous Silicon,*Cambridge University Press, Cambridge **1991**.
[89] S. De Wolf, J. Holovsky, S.-J. Moon, P. Löper, B. Niesen, M. Ledinsky, F.-J. Haug, J.-H. Yum, C. Ballif, *J. Phys. Chem. Lett.* **2014**, *5*, 1035.
[90] B. J. Walker, A. J. Musser, D. Beljonne, R. H. Friend, *Nat. Chem.* **2013**, *5*, 1019.
[91] B. De Geyter, A. J. Houtepen, S. Carrillo, P. Geiregat, Y. Gao, S. ten Cate, J. M. Schins, D. Van Thourhout, C. Delerue, L. D. A. Siebbeles, Z. Hens, *ACS Nano* **2012**, *6*, 6067.
[92] K. E. Knowles, M. Tagliazucchi, M. Malicki, N. K. Swenson, E. A. Weiss, *J. Phys. Chem. C* **2013**, *117*, 15849.
[93] J. T. Stewart, L. A. Padilha, M. M. Qazilbash, J. M. Pietryga, A. G. Midgett, J. M. Luther, M. C. Beard, A. J. Nozik, V. I. Klimov, *Nano Lett.* **2012**, *12*, 622.
[94] J. Mooney, M. M. Krause, J. I. Saari, P. Kambhampati, *J. Chem. Phys.* **2013**, *138*, 204705.
[95] G. Nair, S. Geyer, L.-Y. Chang, M. Bawendi, *Phys. Rev. B* **2008**, *78*, 125325.
[96] M. T. Trinh, A. J. Houtepen, J. M. Schins, T. Hanrath, J. Piris, W. Knulst, A. P. L. M. Goossens, L. D. A. Siebbeles, *Nano Lett.* **2008**, *8*, 1713.
[97] R. Schaller, V. Klimov, *Phys. Rev. Lett.* **2004**, *92*, 186601.
[98] H. Liu, P. Guyot-Sionnest, *J. Phys. Chem. C* **2010**, *114*, 14860.
[99] P. J. Jadhav, A. Mohanty, J. Sussman, J. Lee, M. A. Baldo, *Nano Lett.* **2011**, *11*, 1495.
[100] M. W. B. Wilson, A. Rao, J. Clark, R. S. S. Kumar, D. Brida, G. Cerullo, R. H. Friend, *J. Am. Chem. Soc.* **2011**, *133*, 11830.
[101] N. Zhao, T. P. Osedach, L.-Y. Chang, S. M. Geyer, D. Wanger, M. T. Binda, A. C. Arango, M. G. Bawendi, V. Bulovic, *ACS Nano* **2010**, *4*, 3743.
[102] C. G. Shuttle, B. O'Regan, A. M. Ballantyne, J. Nelson, D. D. C. Bradley, J. de Mello, J. R. Durrant, *Appl. Phys. Lett.* **2008**, *92*, 093311.
[103] M. Argeri, A. Fraccarollo, F. Grassi, L. Marchese, M. Cossi, *J. Phys. Chem. C* **2011**, *115*, 11382.

DOI: 10.1002/adfm.201401816